



## Vertical nonpolar growth templates for light emitting diodes formed with GaN nanosheets

Ting-Wei Yeh,<sup>1,2</sup> Yen-Ting Lin,<sup>1,3</sup> Byungmin Ahn,<sup>2</sup> Lawrence S. Stewart,<sup>1,3</sup> P. Daniel Dapkus,<sup>1,2,3,a)</sup> and Steven R. Nutt<sup>2</sup>

<sup>1</sup>Center for Energy Nanoscience, University of Southern California, Los Angeles, California 90089, USA

<sup>2</sup>Mork Family Department of Chemical Engineering and Materials Science, University of Southern California, Los Angeles, California 90089, USA

<sup>3</sup>Ming Hsieh Department of Electrical Engineering, University of Southern California, California 90089, USA

**Abstract:** We demonstrate that nonpolar *m*-plane surfaces can be generated on uniform GaN nanosheet arrays grown vertically from the (0001)-GaN bulk material. InGaN/GaN multiple quantum wells (MQWs) grown on the facets of these nanosheets are demonstrated by cross-sectional transmission electron microscopy. Owing to the high aspect ratio of the GaN nanosheet structure, the MQWs predominantly grow on nonpolar GaN planes. The results suggest that GaN nanosheets provide a conduction path for device fabrication and also a growth template to reduce the piezoelectric field inside the active region of InGaN-based light emitting diodes. VC 2012 American Institute of Physics. [doi:10.1063/1.3671182]



$\text{In}_{1-x}\text{Ga}_x\text{N}$  is used with GaN to form the multiple quantum wells (MQW) active region of blue/green light emitting diodes (LEDs). Owing to the lattice mismatch between GaN and InGaN, the strain-induced piezoelectric fields inside the MQWs result in the spatial separation of the electron and hole wavefunctions and reduced radiative recombination efficiency with increasing well width; consequently, thin quantum wells, approximately 3 nm thick, are grown to increase the radiative recombination efficiency.<sup>1,2</sup> The thin wells cause inefficient electron capture and high carrier concentrations at the required operating current that can lead to Auger recombination. Both of these effects have been implicated in the high current efficiency “droop” observed in blue and green LEDs.<sup>3,4</sup> Growth on nonpolar or semipolar GaN substrates has been explored as an approach to increase the radiative recombination efficiency in the active region of InGaN/ GaN LEDs by reducing the piezoelectric field and increasing the quantum well thickness.<sup>5-7</sup> However, the cost of these high quality specialized substrates has prohibited widespread adoption. Recently, GaN nanostructures have been studied to exploit their promising properties, including large surfacetovolume ratio and the exposure of facets other than the typical polar (0001), basal plane.<sup>8,9</sup> For example, nanowires are grown on easily accessible substrates by either of two approaches: vapor-liquid-solid growth (VLS) or selective area growth (SAG) by metal organic chemical vapor deposition (MOCVD).<sup>8,9</sup>

In this work, GaN nanosheets that are confined by two parallel {1-100} planes are formed by applying a pulsed GaN SAG growth mode in a close-coupled showerhead MOCVD system using GaN bulk material patterned with a dielectric mask containing <11-20>-oriented stripe openings. InGaN/GaN MQWs are then grown on these nanostructures by changing the growth scheme from pulsed to continuous injection of the gas flux resulting in nanostructures with MQWs predominantly grown on the exposed GaN nonpolar surface. By virtue of their linearly connected structure, GaN



nanosheets provide a continuous electrically conducting path to the active region and enable a three dimension LED active region area larger than the chip area.

Trimethylgallium (TMG) and ammonia ( $\text{NH}_3$ ) were used as the precursors for GaN nanosheet growth at 970 °C. The growth pressure was 200 Torr for the entire pulsed growth mode process. The flow rates of TMG and  $\text{NH}_3$  were 8.8  $\mu\text{mol}/\text{min}$  and 67.0  $\text{mmol}/\text{min}$ , respectively. InGaN/GaN MQWs were grown subsequently on the GaN nanosheets using trimethylindium (TMI) and triethylgallium (TEG) as precursors as the indium and gallium sources, respectively. The flow rates of TEG, TMI, and  $\text{NH}_3$  were 20.0  $\mu\text{mol}/\text{min}$ , 17.0  $\mu\text{mol}/\text{min}$ , and 223.2  $\text{mmol}/\text{min}$ . The growth pressure was increased to 300 Torr in a nitrogen ambient to grow the InGaN quantum wells at 800 °C.

The surface morphology of GaN nanosheet arrays was investigated by field emission scanning electron microscopy (FESEM). Figure 1(a) shows that the resulting nanostructure exhibits long parallel sidewalls that are identified as the nonpolar  $\{1-100\}$  planes. An aspect ratio greater than two is demonstrated under the pulsed growth conditions employed. The relatively small surface areas of polar and semipolar planes in the nanosheets are indicated in Fig. 1(b). Semipolar or nonpolar planes have also been demonstrated in micrometer-scale stripe structures grown by modulating  $\text{NH}_3$  injection to enhance lateral growth.<sup>10,11</sup> The alternate introduction of TMG and then ammonia is called a growth cycle in the pulsed growth mode. Figures 1(c) and 1(d) show the nanosheets after growth for 120 and 240 cycles, respectively. In Fig. 1(c), the width of the nanosheet is 192 nm and the height is 295 nm. After doubling the number of growth cycles, the width increased to 255 nm and the height increased to 524 nm for these growths. Doubling the number of growth cycles resulted in less than double the height but the volume was increased by a factor of two, which is caused by lateral growth occurring on the  $\{1-100\}$  sidewalls.

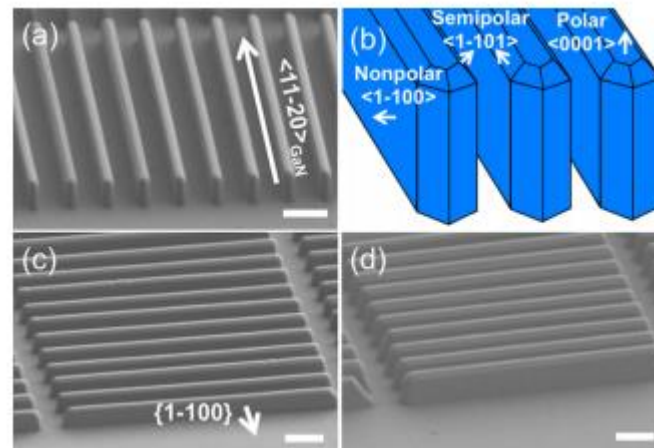


FIG. 1. (Color online) (a) A uniform nanosheet array with 500 nm center-to-center spacing grown on a GaN/Al<sub>2</sub>O<sub>3</sub> buffer layer patterned with a stripe patterns. (b) Polar, semipolar, and nonpolar planes are indicated in the schematic diagram of GaN nanosheets. (c) FESEM image taken with the sample rotated 90 with respect to (a). The nanosheets show vertical and parallel sidewalls, which are {1-100} planes. (d) A nanosheet array grown for double the growth cycles of (c). Each of the FESEM images was recorded at a 60 angle. The scale bar is 500 nm in all figures.

Electron beam lithography was used in this work to define the stripe patterns and to explore the orientation-dependent growth of the nanosheets. In particular, the dependence of the lateral and vertical growth rate as a function of small angular misalignment to the  $\langle 11-20 \rangle$  direction helped to define the sensitivity of the structure shape to the alignment. The design of the stripe patterns nominally aligned to the  $\langle 11-20 \rangle_{\text{GaN}}$  was intentionally varied in the range of  $\pm 3^\circ$  to test this sensitivity. The exaggerated illustration showing the approach to estimate angles and widths from the FESEM top view images of nanosheets is illustrated in the upper left corner of Fig. 2(a). Some representative topview images are also included. The red dotted line is a linear fit to these data, yielding a slope of  $\sim 60$  nm/deg. The y-intercept of the fitted curve showed a minimum width of approximately 131 nm would be achieved if the mask orientation was aligned exactly to  $\langle 11-20 \rangle_{\text{GaN}}$ . This corresponds to the designed width of the stripe pattern. The dependence of the nanosheet width on the orientation of the growth mask indicates that the width of the nanosheet can be controlled either by the width of the design pattern or by the misorientation angle. The height and shape of the



nanosheet is related to the stripe orientation as well. This will be discussed in another paper under preparation. Unless specified the data presented below are taken on samples aligned to within  $\pm 0.5^\circ$ .

To observe the evolution of the nanosheet as the growth proceeds, an experiment was conducted by varying the number of growth cycles on samples with different stripe orientations on the mask, and the results are shown in Fig. 2(b). These results are interpreted to indicate that a larger deviation from the  $\langle 11-20 \rangle_{\text{GaN}}$  orientation results in the formation of more growth steps on the sidewalls of the nanosheets in the early growth stage. As a result, the lateral growth increased dramatically in the misoriented nanosheets within the first 60 growth cycles. The growth steps on the sidewalls diminished as the sidewalls became parallel to the  $\{1-100\}$  nonpolar planes, resulting in a saturation of the lateral growth, especially for nanosheets with larger misorientation.

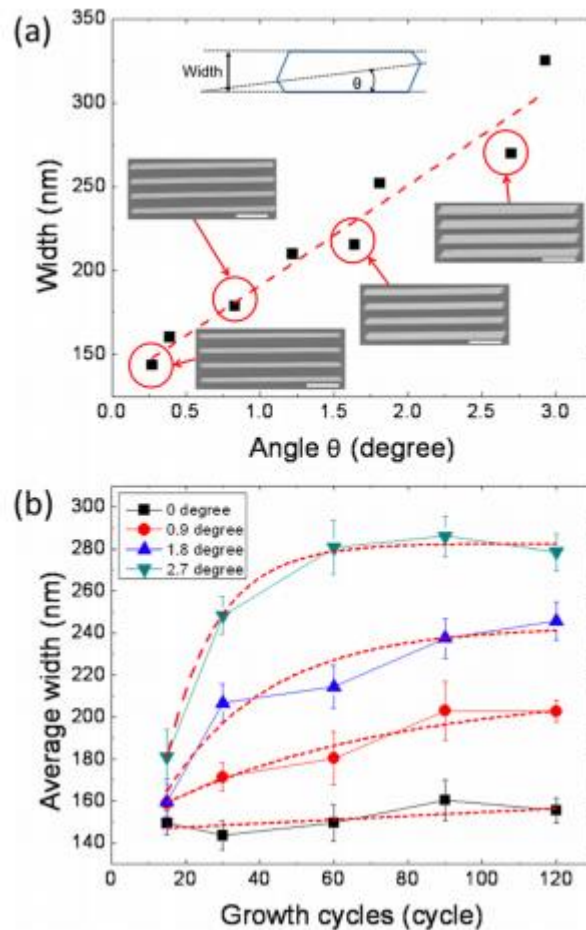


FIG. 2. (Color online) (a) The nanosheet width shows angle-dependent lateral growth within the small range of misoriented patterns. The scale bar is  $1 \mu\text{m}$  in all SEM top view images. (b) Average width of nanosheets as a function of the number of growth cycles is dependent on the orientation of the stripe opening on the mask. The error bar is the standard deviation from the measured result.

In Fig. 3, a cross sectional TEM bright field image is shown of a nanosheet aligned to the  $\langle 11-20 \rangle_{\text{GaN}}$  direction on which three pairs of InGaN/GaN MQWs were grown. The exposure of three main facets in the nanosheet resulted in different growth rates on the various planes. Figure 3(b) also designates the regions where MQWs grew on polar, semipolar, and nonpolar planes, as show in Figs. 3(c)–3(e), respectively. The growth rates of MQWs on each plane resulted in the following sequence: polar (0001) > nonpolar  $\{1-100\}$  > semipolar  $\{1-101\}$ . The QWs grown on the cplane shown in Fig.



3(c) are considerably thicker than typically used for efficient light emitters and result in poor emission efficiency due to the large spatial separation between electron and hole wavefunctions. Furthermore, we observe that the interface between well and barrier is not as abrupt as for other orientations presumably due to the fast growth rate on the c-plane and possibly due to migration of species from the slow growth semipolar facet. In Fig. 3(d), we observe that the MQWs grown on semipolar planes are extremely thin—perhaps too thin to capture the electrons and holes for radiative recombination.

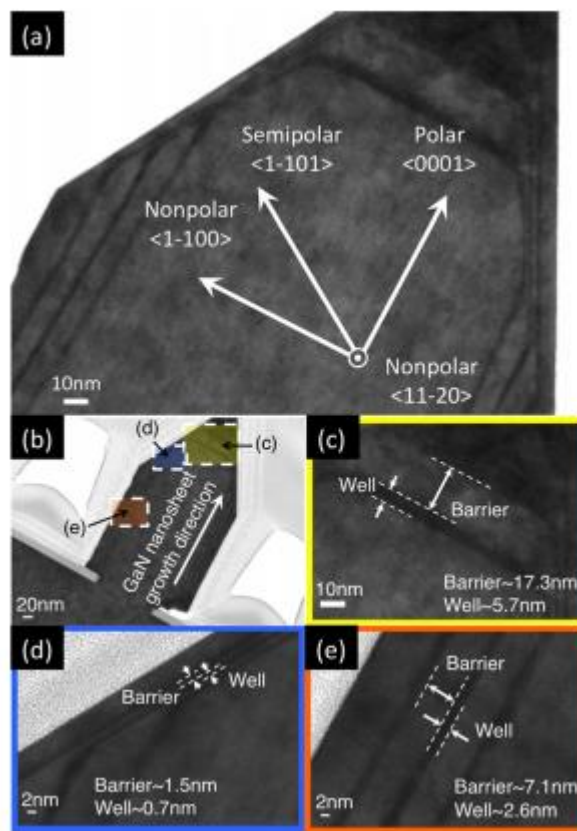


FIG. 3. (Color online) TEM bright field images taken from a sectioned nanosheet with MQWs. (a) InGaN/GaN MQWs were grown on three different planes as indicated in the arrows. (b) A vertical GaN nanosheet grown from its bulk material is shown in the low magnification image. The magnified images taken in (c)-(e) are indicated in (b). Nanosheet surface was covered with carbon to prevent ion beam damage during sample preparation. (c) TEM image shows thick MQWs are grown on the c-plane, polar plane. (d) Thin MQWs are grown on the semipolar plane. (e) MQWs are grown on the nonpolar plane.



Light emission from the MQWs is confirmed by photoluminescence (PL) measurements, as shown in Fig. 4. A dominant QW emission peak, around 436 nm, and a peak from the GaN band edge are clearly observed in the spectrum. A typical defect emission, around 550 nm, is also observed in the figure, which may come from the underlying GaN bulk or GaN nanosheets or both. The inset of Fig. 4 shows a slight decrease in peak wavelengths of the QW emission with increasing mask misorientation, possibly the result of the independence of the nonpolar surface area on the orientation of the stripe described earlier. To confirm the origin of the PL emission, the gaps between nanosheets were filled with hydrogen silsesquioxane to protect the MQWs grown on nonplanar planes. MQWs grown on c-plane and semipolar planes were selectively etched away using inductively coupled plasma reactive ion etching. The PL result was almost identical to that before etching indicating that the light emission is predominantly from the MQWs grown on nonpolar planes.

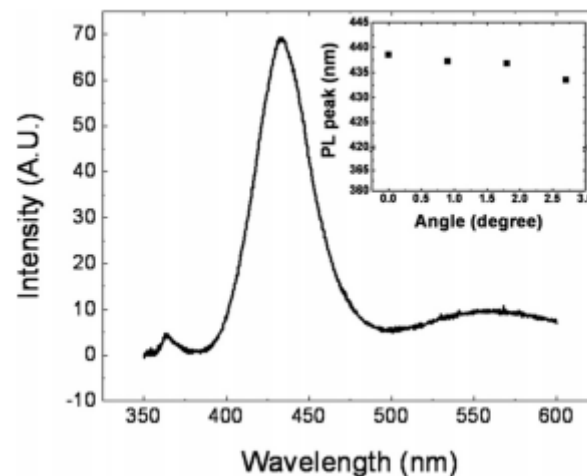


FIG. 4. Room temperature photoluminescence measured from InGaN/GaN MQWs grown on GaN nanosheet arrays.

Large nonpolar GaN surface areas are present in uniform GaN nanosheet arrays grown vertically from the GaN bulk material which serves as a growth template for InGaN/ GaN MQWs. The width



and height of GaN nanosheets are closely related to the misorientation of the stripe opening of the dielectric masks on which the nanosheets are grown. InGaN/GaN MQWs grown on polar, semipolar, and nonpolar planes are revealed by cross-sectional TEM analysis. The strong PL peak indicates that the nonpolar planes of GaN nanosheets are potential candidates for InGaN/GaN MQW growth to reduce the piezoelectric fields inside the active regions of light emitting diodes. The aspect ratio of wellaligned nanosheets may also allow the fabrication of LEDs with large three-dimensional active areas per chip area that may help to further mitigate efficiency droop in LEDs.

**Acknowledgements:** This work was supported in part by NSF through Award ECS-0507270 (TWY) and by the Center for Energy Nanoscience, an Energy Frontier Research Center funded by the U.S. Department of Energy, Office of Basic Energy Sciences under Award Number DE-SC0001013 (Y.T.L., L.S.S., and P.D.D.).

#### **References:**

- <sup>1</sup> E. Berkowicz, D. Gershoni, G. Bahir, E. Lakin, D. Shilo, E. Zolotoyabko, A. C. Abare, S. P. DenBaars, and L. A. Coldren, *Phys. Rev. B* 61(16), 10994 (2000).
- <sup>2</sup> J. Bai, T. Wang, and S. Sakai, *J. Appl. Phys.* 88(8), 4729 (2000).
- <sup>3</sup> Y. C. Shen, F. O. Muller, S. Watanabe, N. F. Gardner, A. Munkholm, and M. R. Krames, *Appl. Phys. Lett.* 91, 141101 (2007).
- <sup>4</sup> M.-H. Kim, M. F. Schubert, Q. Dai, J. K. Kim, E. F. Schubert, J. Piprek, and Y. Park, *Appl. Phys. Lett.* 91, 183507 (2007).
- <sup>5</sup> A. Chakraborty, B. A. Haskell, S. Keller, J. S. Speck, S. P. DenBaars, S. Nakamura, and U. K. Mishra, *Jpn. J. Appl. Phys.* 44(5), L173 (2005).
- <sup>6</sup> M. Funato, M. Ueda, Y. Kawakami, Y. Narukawa, T. Kosugi, M. Takahashi, and T. Mukai, *Jpn. J. Appl. Phys.* 45(26), L659 (2006).
- <sup>7</sup> H. Zhong, A. Tyagi, N. N. Fellows, F. Wu, R. B. Chung, M. Saito, K. Fujito, J. S. Speck, S. P. DenBaars, and S. Nakamura, *Appl. Phys. Lett.* 90, 233504 (2007).
- <sup>8</sup> X. Duan and C. M. Lieber, *J. Am. Chem. Soc.* 122, 188 (2000).
- <sup>9</sup> S. D. Hersee, X. Sun, and X. Wang, *Nano Lett.* 6(8), 1808 (2006).
- <sup>10</sup> X. Zhang, P. D. Dapkus, and D. H. Rich, *Appl. Phys. Lett.* 77, 1496 (2000).
- <sup>11</sup> R. S. Q. Fareed, J. W. Yang, J. Zhang, V. Adivarahan, V. Chaturvedi, and M. A. Khan, *Appl. Phys. Lett.* 77, 2343 (2000).